DAVID W. TAYLOR NAVAL SHIP RESEARCH AND DEVELOPMENT CENTER

Bethesda, Md. 20084

A COMPARISON BETWEEN THE DRAGS PREDICTED BY BOUNDARY-LAYER THEORY AND EXPERIMENTAL DRAG DATA FOR BODIES OF REVOLUTION

by

Nadine M. White

Final rept.

APPROVED FOR PUBLIC RELEASE: DISTRIBUTION UNLIMITED

31 p.

SHIP PERFORMANCE DEPARTMENT
DEPARTMENTAL REPORT

AUG 1977

SPD-784-01

A COMPARISON BETWEEN THE DRAGS PREDICTED BY BOUNDARY-LAYER THEORY AND EXPERIMENTAL DRAG DATA FOR BODIES OF REVOLUTION by Nadine M. White SPD-784-01

MAJOR DTNSRDC ORGANIZATIONAL COMPONENTS

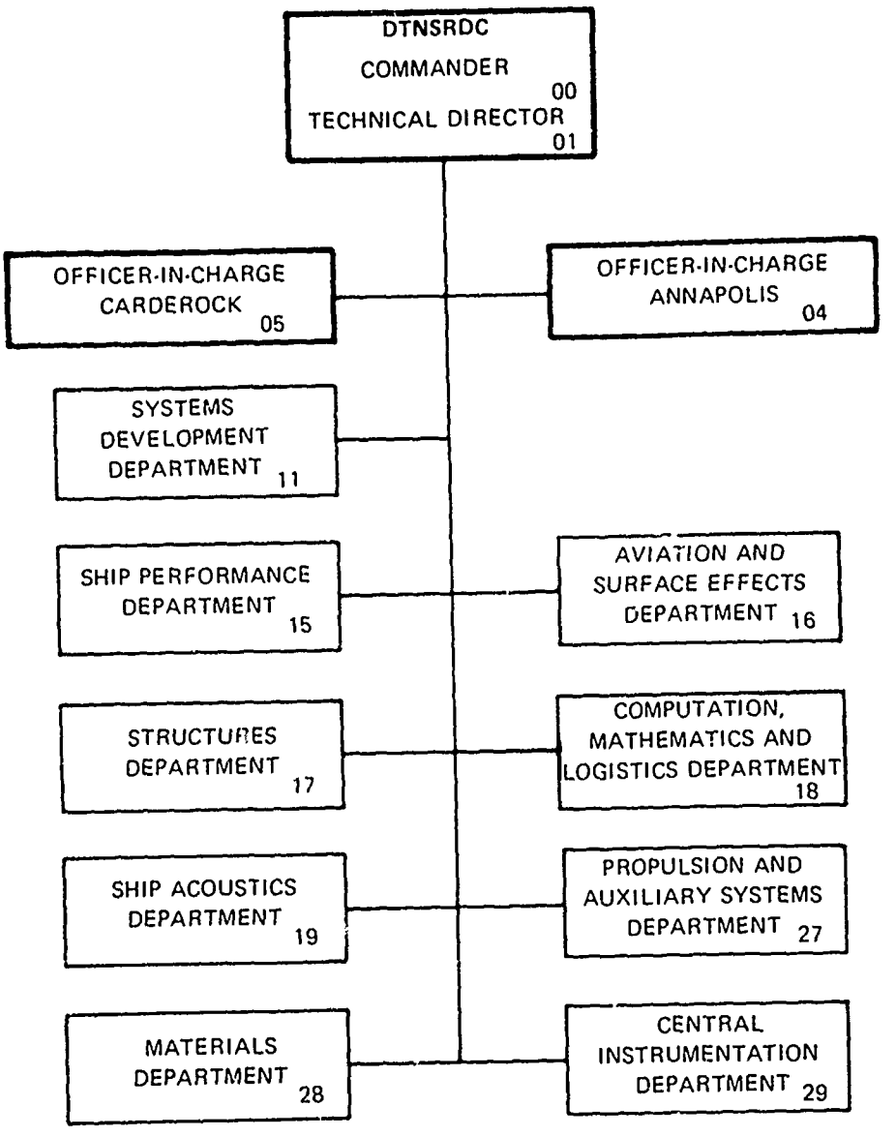

UNCLASSIFIED

SECURITY CLASSIFICATION OF THIS PAGE *(When Data Entered)*

REPORT DOCUMENTATION PAGE		READ INSTRUCTIONS BEFORE COMPLETING FORM
1. REPORT NUMBER SPD-784-01	2. GOVT ACCESSION NO.	3. RECIPIENT'S CATALOG NUMBER
4. TITLE *(and Subtitle)* A Comparison Between the Drags Predicted by Boundary-Layer Theory and Experimental Drag Data for Bodies of Revolution		5. TYPE OF REPORT & PERIOD COVERED Final 6. PERFORMING ORG. REPORT NUMBER
7. AUTHOR(s) Nadine M. White		8. CONTRACT OR GRANT NUMBER(s)
9. PERFORMING ORGANIZATION NAME AND ADDRESS David W. Taylor Naval Ship R&D Center Bethesda, MD 20084		10. PROGRAM ELEMENT, PROJECT, TASK AREA & WORK UNIT NUMBERS WR N651 777WR75684 Work Unit 1552-136
11. CONTROLLING OFFICE NAME AND ADDRESS Naval Ship Engineering Center Washington, DC 20362		12. REPORT DATE August 1977 13. NUMBER OF PAGES 26
14. MONITORING AGENCY NAME & ADDRESS*(if different from Controlling Office)*		15. SECURITY CLASS. *(of this report)* UNCLASSIFIED 15a. DECLASSIFICATION/DOWNGRADING SCHEDULE

16. DISTRIBUTION STATEMENT *(of this Report)*

APPROVED FOR PUBLIC RELEASE: DISTRIBUTION UNLIMITED

17. DISTRIBUTION STATEMENT *(of the abstract entered in Block 20, if different from Report)*

18. SUPPLEMENTARY NOTES

19. KEY WORDS *(Continue on reverse side if necessary and identify by block number)*

20. ABSTRACT *(Continue on reverse side if necessary and identify by block number)*

A finite-difference method used by Wang and Huang to predict the drag coefficients of axisymmetric bodies is systematically applied to eight series of model forms comprising nearly fifty bodies. Calculations of residual drag are compared to available experimental data in order to determine the usefulness of the method for predictive purposes. The method is shown to exhibit little sensitivity to changes in nose or tail radii or prismatic coefficient. The

over

DD FORM 1 JAN 73 1473 EDITION OF 1 NOV 65 IS OBSOLETE
S/N 0102-014-6601

UNCLASSIFIED

SECURITY CLASSIFICATION OF THIS PAGE *(When Data Entered)*

method does exhibit the ability to correctly predict drag trends for variations in length-to-diameter ratio, entrance-length-to-diameter ratio, and tail-length-to-diameter ratio.

TABLE OF CONTENTS

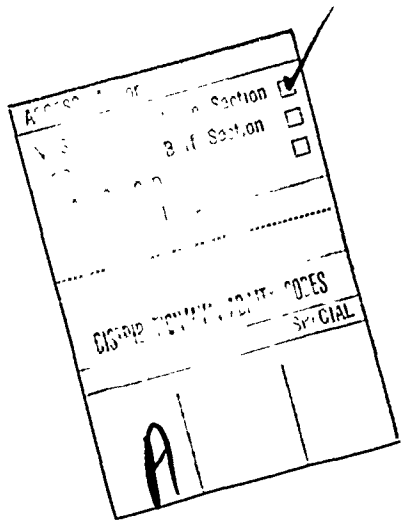

ABSTRACT

A finite-difference method used by Wang and Huang to predict the drag coefficients of axisymmetric bodies is systematically applied to eight series of model forms comprising nearly fifty bodies. Calculations of residual drag are compared to available experimental data in order to determine the usefulness of the method for predictive purposes. The method is shown to exhibit little sensitivity to changes in nose or tail radii or prismatic coefficient. The method does exhibit the ability to correctly predict drag trends for variations in length-to-diameter ratio, entrance-length-to-diameter ratio, and tail-length-to-diameter ratio.

ADMINISTRATIVE INFORMATION

This work was authorized and funded by the Naval Ship Engineering Center, under work request number N651 777WR75684, internal job order number 1552-136.

INTRODUCTION

In a recent report[1] by Wang and Huang, a description is given of a computer program which calculates the incompressible boundary layer flow and pressure distribution over an axisymmetric body in uniform flow at zero angle of attack. The method, based on the theory of Cebeci and Smith,[2,3] calculates viscous flow over a body using a differential boundary-layer formulation in conjunction with the integral wake relations given by Granville.[4] The resulting displacement thicknesses are then used to generate a new overall body-wake displacement model. An iteration loop calculates a new boundary-layer flow over the body until successive pressure distributions agree to

---

[1] Wang, H.T. and T.T. Huang, "User's Manual For a FORTRAN IV Computer Program for Calculating the Potential Flow/Boundary Layer Interaction on Axisymmetric Bodies," DTNSRDC SPD-737-01 (Dec 1976).

[2] Cebeci, T., G.J. Mosinskis, and A.M.O. Smith, "Calculation of Viscous Drag and Turbulent Boundary-Layer Separation on Two-Dimensional and Axisymmetric Bodies in Incompressible Flows," Douglas Aircraft Company Report MDC-J0973-01 (Nov 1970).

[3] Cebeci, T., G.J. Mosinskis, and L.C. Wang, "A Finite Difference Method for Calculating Compressible Laminar and Turbulent Boundary Layers, Part II-User's Manual" Douglas Aircraft Co. Report DAC-67131 (May 1969).

[4] Granville, P.S., "The Calculation of the Viscous Drag of Bodies of Revolution," DTMB Report 849 (Jul 1953).

within a specified error criterion or until the specified maximum number of iterations is reached. The total drag coefficient, C_D, is normalized on wetted area and dynamic head. C_R, the residual drag coefficient, is calculated by subtracting off the frictional drag, C_f, from C_D. C_f is calculated using the ITTC line which provides a flat-plate equivalent drag for each body of revolution.

Figure 1 gives a sketch of a typical axisymmetric body, the body wake displacement surface and the definition of coordinate system used by the program in the calculation loop.

The computer user's manual of reference 1 lists only one sample case for program checkout use. Reference 5 presents comparisons of theoretical predictions with experimental data for three axisymmetric bodies. Reference 2 presents experimental and calculated drag values for 10 airfoils. The present study attempts to investigate more thoroughly the drag-prediction capabilities of the method of reference 1 by testing nearly 50 axisymmetric bodies for which experimental drag data are available. It was hoped that, at the least, the same order of "drag merit" as that measured experimentally would be predicted. Even if the drag coefficients are not in close numerical agreement, the method might be useful as a relative indicator of drag characteristics.

This study was conducted in the aftermath of an extensive survey presented in reference 6. In the earlier report, most of the same 50 bodies presented here were used tc check the predictive capability of a simple drag formula currently in use. It was found that the simple formula was not consistent enough to be used for predictive purposes and that better prediction methods were required. The finite-difference method which is studied here provides a much more detailed calculation of boundary-layer development.

OUTLINE OF COMPUTATIONS

Point-generating computer programs were developed to give an accurate physical representation of each body surface for computer use. The creation of these point distributions usually involved using the model's original drawings or offsets to provide a fairly accurate curve. Fairing polynomials

[5]Huang, T.T., et al, "Propeller/Stern/Boundary Layer Interaction on Axisymmetric [6]Bodies: Theory and Experiment," DTNSRDC Report 76-0113 (Dec 1976).
[6]White, N.M., "A Comparison Between a Simple Drag Formula and Experimental Drag Data for Bodies of Revolution", DTNSRDC report 77-0028 (Jan 1977).

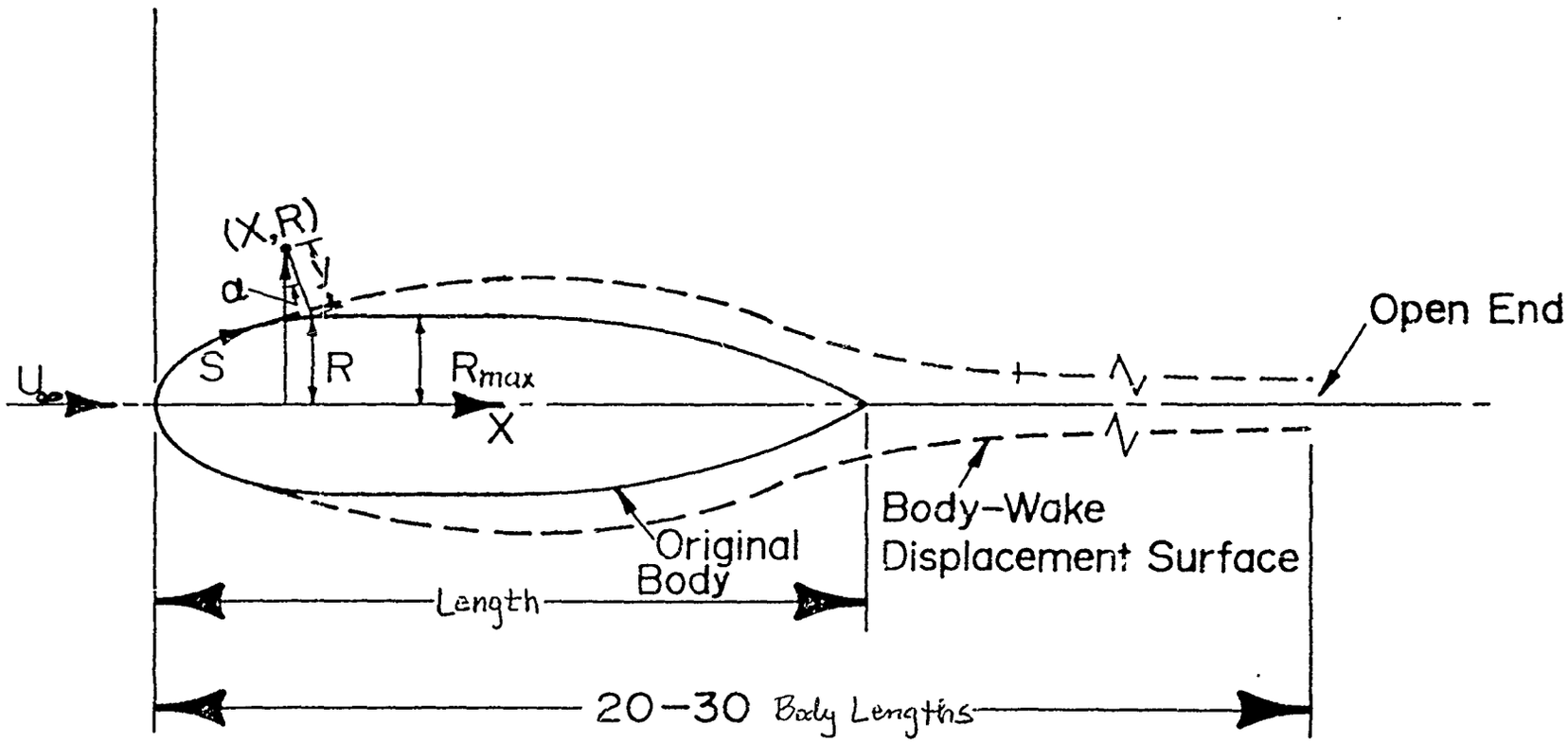

Figure 1—Definition Sketch of Original Body and Body-Wake Displacement Surface

based on a least-squares fit were then passed through the data points to insure smooth rates of change in R. All model point distributions were then scaled to a uniform length of 10 feet (3.048 m) for the computer drag calculation. All drag calculations were done at a model-scale Reynolds number of 20×10^6, and the location of transition was fixed at 1.5% of body length. Comparisons were made on the basis of the residual-drag coefficient, C_R, which for a deeply submerged body is a form (or pressure) drag coefficient.

Additional comparisons are also made with drag computations for the same bodies based on the simple drag formula studied by White.[6] This formula combines an empirically determined power-law formula with potential-flow computations to give a total drag coefficient C_D defined by

$$C_D = \frac{2\pi L^2 C_f}{A} \int_0^1 \left(\frac{R}{L}\right)^{7/6} \left(\frac{u}{u_\infty}\right)^{10/3} \sec\alpha \, d\left(\frac{x}{L}\right)^{6/7}$$

with $C_R = C_D - C_f$, where C_f is the equivalent flat-plate drag for each body of revolution. The results of this earlier study will be repeated here to allow direct correlations to be made with another available drag-computation method as well as a comparison with experimentally derived data.

RESULTS

Eight series of bodies were used to test the computer program of Reference 1:

(1) the Series 58 bodies investigated by Gertler,[7]

(2) Series 5242 stern forms (unpublished),

(3) a series of bodies based on the best Series 58 model with various amounts of parallel middle body as reported by Larsen,[8]

---

[7] Gertler, Morton, "Resistance Experiments on a Systematic Series of Streamlined Bodies of Revolution - For Application to the Design of High Speed Submarines," DTMB Report C-297 (Apr 1950), declassified 27 Jan 1967.

[8] Larsen, C.A., "Additional Tests of Series 58 Forms, Part 1, Resistance Tests on a Parallel Middle Body Series," DTMB Report C-738 (Nov 1955), declassified 2 Sept 1975.

(4) Series 4620 forebodies investigated by McCarthy, Power, and Huang,[9]

(5) polynomial representation of five miscellaneous models,

(6) Series 4935 afterbodies (unpublished),

(7) six bodies with inflected sinusoidal sterns studied by Kempf[10,11] (referred to herein as "Kempf bodies")

(8) the Series 4620 afterbodies (unpublished).

Except for the Series 4620 afterbodies (series 8), details regarding the shapes of these bodies and appropriate additional references are available in Reference 5. No attempt will be made in this report to evaluate the accuracy of the reported experimental data, some of which may have been subject to error. Comparisons are made only of relative order of merit as found by the various experimenters and as computed by the two methods referred to above.

Series 58

The first series of bodies studied was the Series 58 originally developed by Gertler.[6] Table 1 shows the results for Series 58 ordered by model number. The order of merit shown is relative to the model having the smallest experimental value of C_R.

It is apparent that, for the overall series, the computed orders of merit are quite different from the order of merit derived from model experiments. Correct placement of three bodies is predicted (Models 4154, 4155 and 4176 - all of them having extremely high drag coefficients). In addition, although the same three models (4165, 4159, and 4158) were picked as the three "best" choices by both experiment and the finite-difference scheme, the fourth-best body predicted by the finite-difference method (Model 4164) ranks twenty-second experimentally. In comparison with the simple formula, there is no better agreement with experiment. Six bodies (Models 4154, 4156, 4159, 4166, 4167 and 4175) have their placements predicted correctly. Both of these methods designate Model 4159 as best, the simple formula

[9] McCarthy, J.H., J. Power, and T.T. Huang, "The Roles of Transition, Laminar Separation and Turbulence Stimulation in the Analysis of Axisymmetric Body Drag," Proceedings of the Eleventh ONR Symposium on Naval Hydrodynamics, sponsored by the Office of Naval Research, London (Mar 1976).

[10] Kempf, George, "Resistance and Wake of Bodies of Revolution" from "New Developments in Ship Research", Jahrbuch Schiffbautechnischen Gesellschaft (1927), pp. 177-178.

[11] Kempf, George, "Turbulent Separation on Full Ship Forms," Schiff und Hafen) Vol. 6, no. 7, Hamburg (1954).

TABLE 1

C_R Comparisons for Series 58

Body No.	Experimental $C_R \times 10^3$	Simple Formula $C_R \times 10^3$	Finite Difference Method $C_R \times 10^3$	Experimental Order of Merit	Simple Formula Order of Merit	Finite Difference Method Order of Merit
4154	0.58	0.48	0.40	24	24	24
4155	0.36	0.37	0.33	21	23	21
4156	0.22	0.30	0.27	18	20	20
4157	0.13	0.23	0.23	6	16	7
4158	0.09	0.18	0.19	3	3	2
4159	0.075	0.11	0.15	2	1	1
4160	0.12	0.21	0.23	5	5	11
4161	0.15	0.21	0.23	12	6	8
4162	0.17	0.22	0.23	15	8	10
4163	0.19	0.22	0.23	17	9	12
4164	0.37	0.24	0.22	22	17	4
4165	0.07	0.23	0.21	1	14	3
4166	0.28	0.24	0.25	19	18	18
4167	0.16	0.25	0.25	13	19	19
4168	0.14	0.22	0.24	10	11	16
4169	0.14	0.23	0.23	11	15	6
4170	0.18	0.20	0.22	16	4	5
4171	0.13	0.17	0.24	7	2	13
4172	0.13	0.22	0.23	8	7	9
4173	0.13	0.22	0.24	9	12	14
4174	0.10	0.22	0.24	4	10	17
4175	0.32	0.36	0.33	20	22	22
4176	0.41	0.35	0.34	23	21	23
4177	0.16	0.23	0.24	14	13	15

predicts that Model 4158 is third best while the finite-difference method predicts that it is second best. The second best body according to the simple formula ranks thirteenth according to the finite-difference scheme.

As mentioned in Reference 5 there are several sub-series within the overall model range of Series 58 based on the variation of five nondimensional quantities. The nondimensional quantities used were length-to-diameter ratio, $\lambda = L/D$, axial location of maximum section, $m = x_m/L$, nondimensional nose and tail radii, $r_o = R_o L/D^2$ and $r_1 = R_2 L/D^2$, and the prismatic coefficient, $C_p = 4V/\pi LD^2$. Tables 2, 3, 4, 5, 6 and 7 list the Series 58 bodies involved in these sub-series and compare the experimental and simple formula results with those of the finite-difference method. Figure 2 provides a graphical comparison between the experimental and finite difference values for C_R.

TABLE 2

Series 58 Body Variations in L/D

($m = 0.450$, $C_p = 0.65$, $r_o = 0.5$, $n = 0.1$)

Model Number	L/D	Experimental $C_R \times 10^3$	Simple Formula $C_R \times 10^3$	Finite Difference $C_R \times 10^3$
4154	4.0	0.58	0.48	0.40
4155	5.0	0.36	0.37	0.33
4156	6.0	0.22	0.30	0.27
4157	7.0	0.13	0.23	0.23
4158	8.0	0.09	0.18	0.19
4159	10.0	0.075	0.11	0.15

TABLE 3

Series 58 Body Variation in m, Maximum Thickness Location

($4D = 7.0$, $C_p = 0.65$, $r_o = 0.5$, $r_1 = 0.1$)

Model Number	m.	Experimental $C_R \times 10^3$	Simple Formula$_3$ $C_R \times 10^3$	Finite Difference $C_R \times 10^3$
4177	0.34	0.16	0.23	0.24
4160	0.36	0.12	0.21	0.23
4157	0.40	0.13	0.23	0.23
4161	0.44	0.15	0.21	0.23
4162	0.48	0.17	0.22	0.23
4163	0.52	0.19	0.22	0.23

TABLE 4

Series 58 Body Variation in C_p, the Prismatic Coefficient, for L/D = 7.0

($m = 0.4$, $r_o = 0.5$, $r_1 = 0.1$)

Model Number	C_p	Experimental $C_R \times 10^3$	Simple Formula$_3$ $C_R \times 10^3$	Finite Difference $C_R \times 10^3$
4164	0.55	0.37	0.24	0.22
4165	0.60	0.07	0.23	0.21
4157	0.65	0.13	0.23	0.23
4166	0.70	0.28	0.24	0.25

TABLE 5

Series 58 Body Variation in C_p, the Prismatic Coefficient, for L/D = 5.0

($m = 0.4$, $r_o = 0.5$, $r_1 = 0.1$)

Model Number	C_p	Experimental $C_R \times 10^3$	Simple Formula$_3$ $C_R \times 10^3$	Finite Difference $C_R \times 10^3$
4176	0.55	0.41	0.35	0.34
4175	0.60	0.32	0.36	0.33
4155	0.65	0.36	0.37	0.33

TABLE 6

Series 58 Body Variations in r_o, Nondimensional Nose Radius

($L/D = 7.0$, $C_p = 0.65$, $m = 0.4$, $r_1 = 0.1$)

Model Number	r_o	Experimental $C_R \times 10^3$	Simple Formula$_3$ $C_R \times 10^3$	Finite Difference $C_R \times 10^3$
4167	0.00	0.16	0.25	0.25
4168	0.30	0.14	0.22	0.24
4157	0.50	0.13	0.23	0.23
4169	0.70	0.14	0.23	0.23
4170	1.00	0.18	0.20	0.22

TABLE 7

Series 58 Body Variations in r_1, Nondimensional Tail Radius
($L/D = 7.0$, $C_p = 0.65$, $m = 0.4$, $r_o = 0.5$)

Model Number	r_1	Experimental $C_R \times 10^3$	Simple Formula$_3$ $C_R \times 10^3$	Finite Difference $C_R \times 10^3$
4171	0.00	0.13	0.17	0.24
4172	0.05	0.13	0.22	0.23
4157	0.10	0.13	0.23	0.23
4173	0.15	0.13	0.22	0.24
4174	0.20	0.10	0.22	0.24

The computed values of C_R for the finite-difference method as a function of L/D have the same order of merit as both the experimental values of C_R and those C_R's computed by the simple formula as shown in Table 2. However the computed values of C_R in Tables 3, 4, 5, 6, and 7 indicate that the finite-difference method is as relatively insensitive to changes in m, C_p, r_o and r_1 as the simple formula. For example, Table 3 shows almost no change in the value of C_R for the finite-difference method while the experimental values indicate a moderately strong dependence on m. Similarly, Table 4 indicates a strong dependence on C_p in the experimental data but only a very little difference in C_R is predicted by the finite-difference method.

The only series where consistent trends can be seen in both computed and experimental C_R values is for models where L/D varies (Table 2). Both computational methods and the experimental data indicate a decreasing C_R with increasing L/D. Thus, it is possible that the finite-difference method may be used to identify a poor body occurring when L/D is being varied, but not for variations of the other geometric parameters used here.

Models 5242-1, 2, 3

This series of bodies is based on a common forebody with added sterns of differing fullness. Parallel middle body was added to each afterbody in such a way as to produce three hulls of constant volume. For additional information

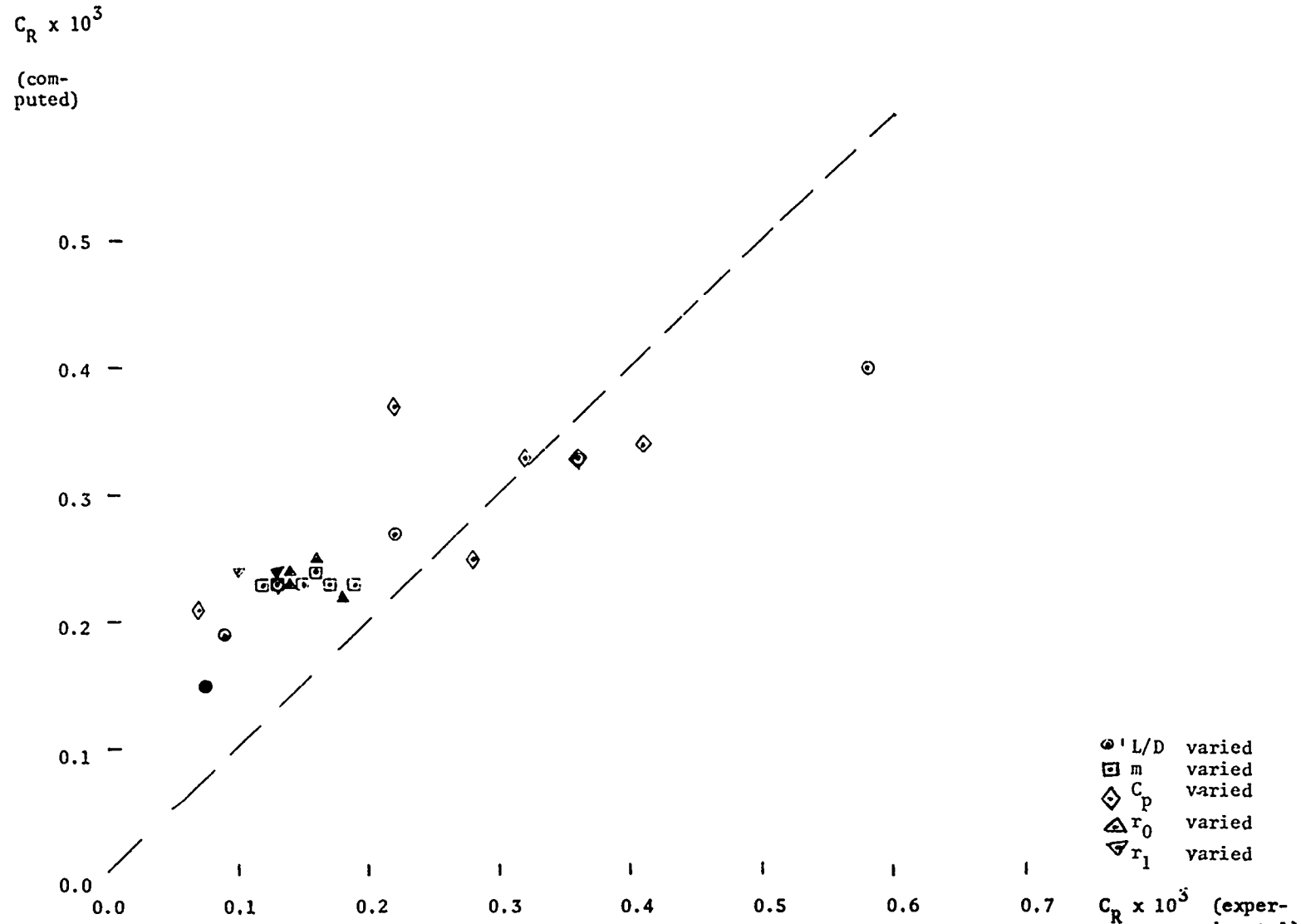

Figure 2. Comparison of Experimental and Finite-Difference-Method C_R Values for Series 58.

on the polynomials used to describe this series, see Reference 5. Table 8 shows experimental results for the Series 5242 models along with C_R's computed using both the finite-difference method and the simple formula. Figure 3 shows a graphical comparison between the finite-difference method C_R's and the experimental data.

TABLE 8

Residual Drag Comparisons for the Series 5242 Models

Model Number	C_p Stern	$L_{R/D}$	Experimental $C_R \times 10^3$	Simple Formula $C_R \times 10^3$	Finite Difference $C_R \times 10^3$
5242-1	0.674	2	0.375	0.23	0.196
5242-2	0.574	3	0.310	0.20	0.165
5242-3	0.505	4	0.255	0.21	0.149

The bare hull data show that C_R increases with decreasing L_R/D. This trend is predicted by the finite-difference method although not by the simple formula. The finite-difference method's C_R's indicate a greater amount of differentiation between models of the series than found by the simple formula but not quite as much of a difference as was found experimentally. The predicted values of C_R are lower than the measured values of C_R, which was only true for the poorest Series 58 bodies. The finite-difference method apparently is sensitive enough to discriminate variations in the parameter L_R/D.

Series 58 Parallel Middle Body Series

The third series of body models studied was based on the experimentally determined "best" model of the Series 58 (Model 4165). The original equation was used to define the geometry of nose and tail with increasing amounts of parallel middle body added to generate a new series of models. The experiments reported by Larsen[7] give data for models having 30, 40, 50, and 60 percent of their lengths in parallel middle body. For additional information and sketches see Reference 5. Results of the drag calculations

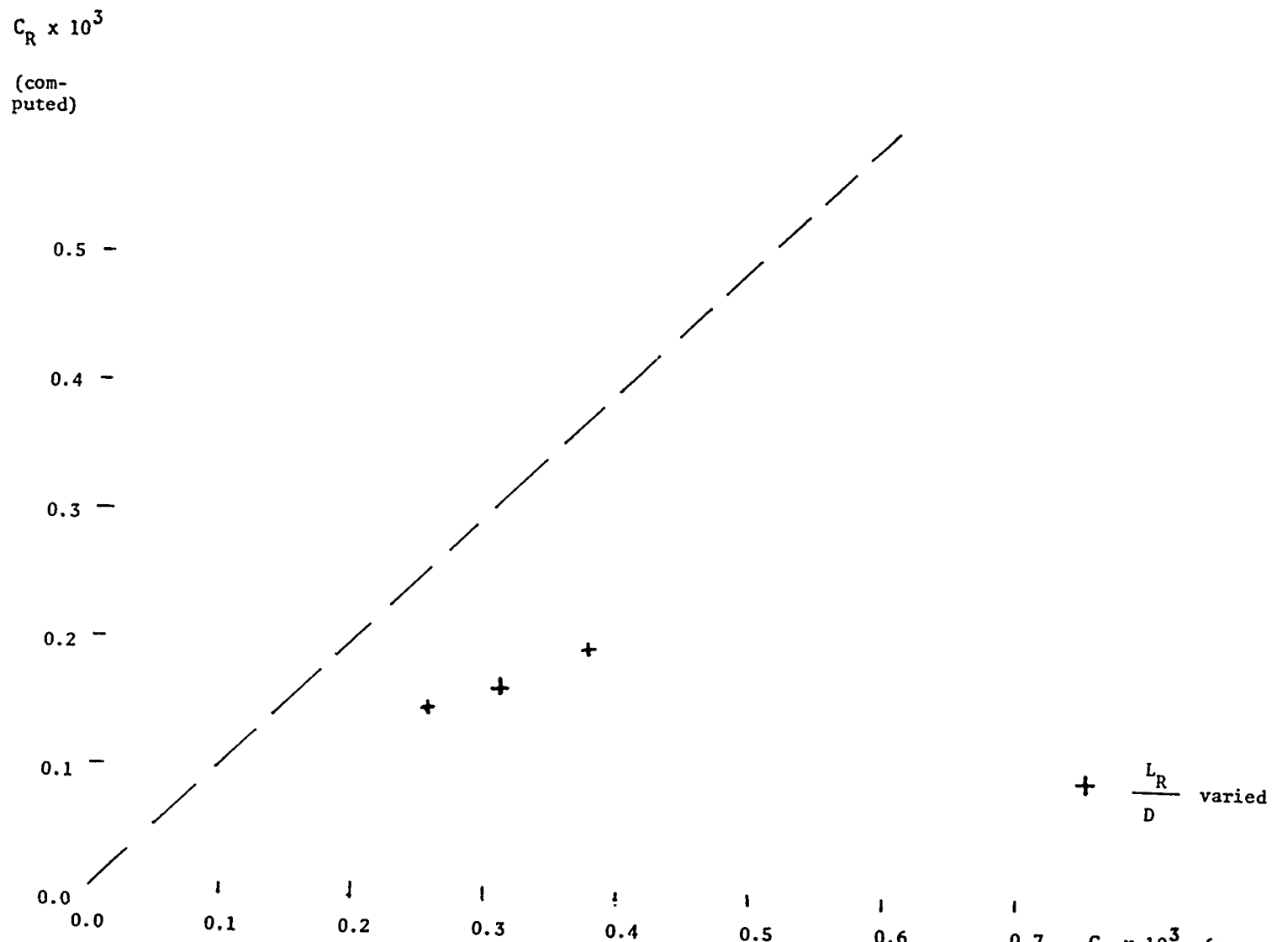

Figure 3. Comparison of Experimental and Finite-Difference-Method C_R Values for Series 5242.

are listed in Table 9 and Figure 4 gives a graphical comparison of the computed C_R's from the finite-difference formula and experimental values of C_R.

TABLE 9

Residual Drag Comparisons for the Series 58 Parallel Middle Body Series (Nose and Tail Shape fixed, maximum diameter fixed)

Model Number	L/D	Experimental $C_R \times 10^3$	Simple Formula $C_R \times 10^3$	Finite Difference $C_R \times 10^3$
4165	7.00	0.07	0.23	0.215
4165-30	10.00	0.10	0.17	0.143
4165-40	11.67	0.12	0.15	0.124
4165-50	14.00	0.14	0.12	0.109
4165-60	17.50	0.15	0.10	0.095

The experimental drag data in Table 9 indicate that C_R values increase with increasing amounts of parallel middle body. Both the finite-difference method and the simple formula show values of C_R decreasing with increasing parallel middle body. This trend in the computed values is consistent with the Series 58 data which showed a similar reduction in the values of C_R for increasing L/D. Both methods stand in disagreement with the experimental data of Larsen.

Series 4620 Forebodies

The parent model for this series provided a common tail form for use with four bodies of revolution whose bow-entrance-length-to-diameter ratios were varied. Model 4620-1 had a hemispherical nose. The other three bodies are described by polynomials. For an extended description of these bodies see Reference 5. Table 10 below contains the results of the C_R computations and Figure 5 has a graphical comparison of the experimental C_R's and those of the finite-difference method.

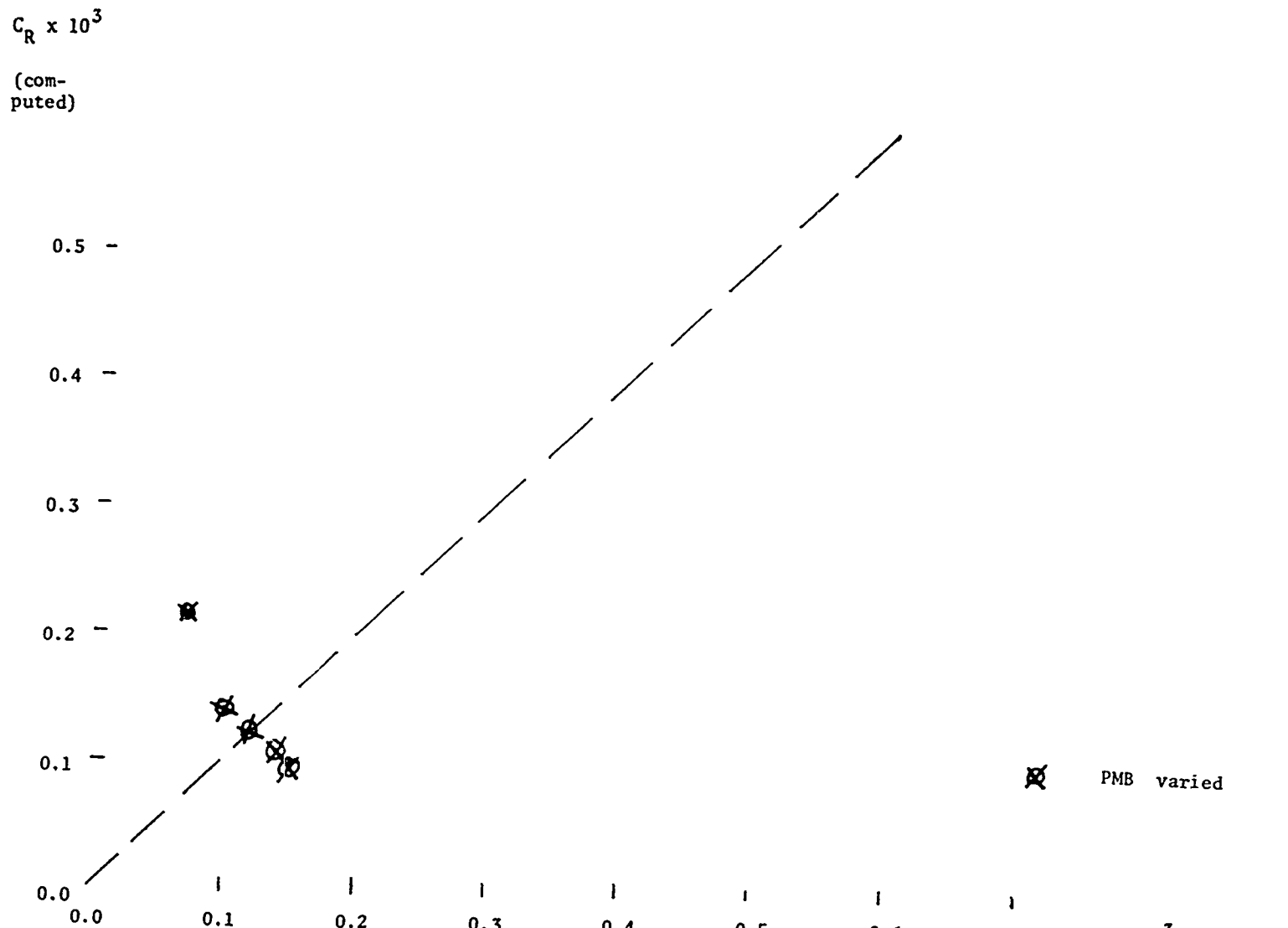

Figure 4. Comparison of Experimental and Finite-Difference-Method C_R Values for Series 58 Parallel-Middle-Body Models.

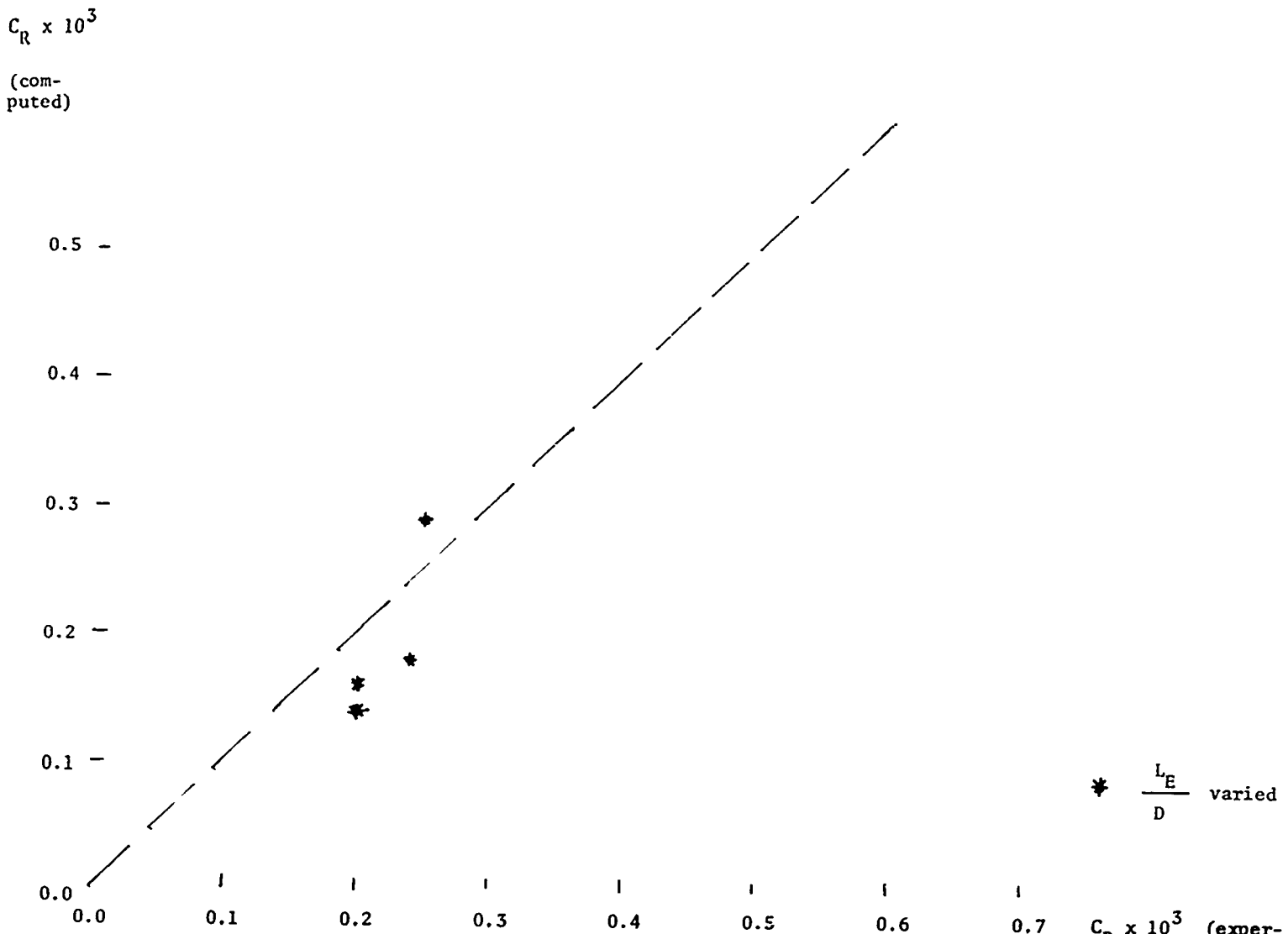

Figure 5. Comparison of Experimental and Finite-Difference-Method C_R Values for Series 4620.

The experimental and computed values of C_R do not agree as to the relative order of merit for this group of bodies. Experimentally, model 4620 was best and Model 5224-1 was the worst. The simple formula predicts that Model 5290 is best, as does the finite-difference method. The finite-difference method fails to see any difference in C_R values for Models 4620, 4935, and 4627, while the experimental data and simple-formula predictions discriminate much more between these models. It should be recalled here that the finite-difference formula did not predict well the overall ordering of the Series 58.

Model 4935 Extended Tail Series

This series of models was based on an existing form represented by Model 4935-1. Extended tail shapes were developed and faired into the original model. The two extended sterns involve a 3.4 and 6.2-percent of full-scale-length tail extension (Models 4935-2 and 3 respectively) which was then smoothed into the original hull approximately 7.5 stations aft of the parallel middle body. Sketches and pressure distributions for these forms may be found in Reference 5. Experimental values of C_R along with the C_R's computed by the two predictive methods are shown in Table 12. Figure 7 graphically compares the finite-difference method values of C_R with the experimental data.

TABLE 12

Residual Drag Comparisons for Model 4935 Extended Tail Series

Model Number	Stern Extension (ft)	Experimental $C_R \times 10^3$	Simple Formula $C_R \times 10^3$	Finite Difference $C_R \times 10^3$
4935-1	0	0.23	0.22	0.18
4935-2	10	0.17	0.22	0.18
4935-3	18	0.13	0.23	0.17

The experimental data show a reduction in C_R with increasing L_R/D. The finite-difference method also follows this trend but only barely discriminates between any of the three models. The simple method fails to discriminate

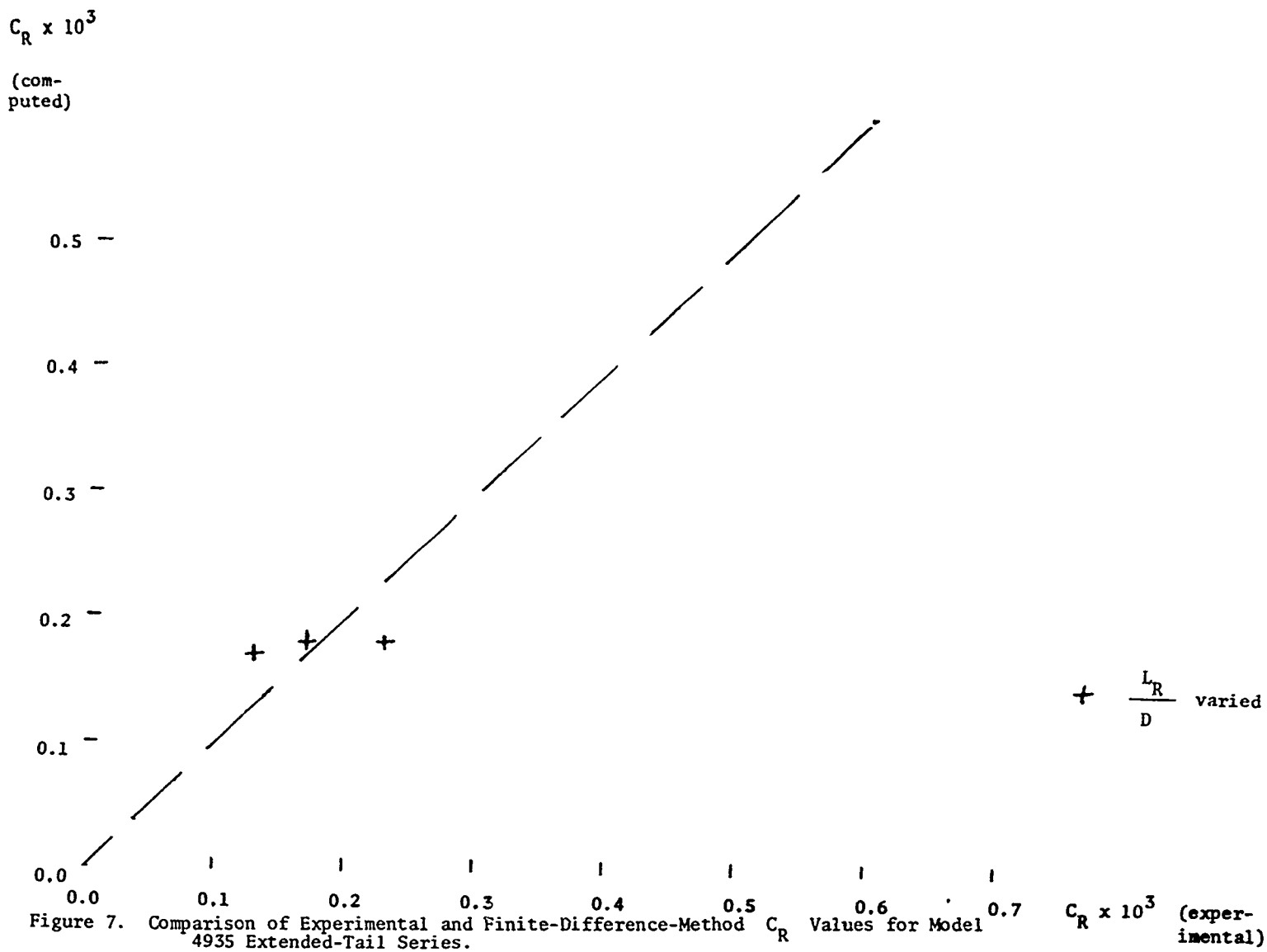

Figure 7. Comparison of Experimental and Finite-Difference-Method C_R Values for Model 4935 Extended-Tail Series.

TABLE 10

Residual Drag Comparisons for Series 4620 Forebodies

Model Number	$L_{E/D}$	Experimental $C_R \times 10^3$	Simple Formula$_3$ $C_R \times 10^3$	Finite Difference $C_R \times 10^3$
4620-1	0.50	0.25	0.22	0.20
4620-2	1.00	0.24	0.17	0.18
4620-3	1.82	0.20	0.14	0.16
4620-4	3.00	0.20	0.12	0.14

Both the measured and predicted values of C_R show the same relative order of merit for this series. In all cases the values of C_R increase with decreasing L_E/D. Both predictive methods, however, show lower values and a greater spread between the values of C_R for these four models.

Miscellaneous Models Series

A fifth group consisting of miscellaneous model hulls fitted with polynomials was investigated. Five models were involved: Model 4620 parent form, Model 4935 parent form, Model 4627, Model 5224-1 and Model 5290. Least squares fit polynomials were used to remove irregularities from drawing offsets and to provide a smooth C_p distribution. Additional information on these models may be found in Reference 5, along with their pressure distributions and other sources. A comparison of the predicted and measured drag coefficients for this series is shown in Table 11 and a graphical comparison of the C_R's obtained is shown in Figure 6.

TABLE 11

Residual Drag Comparisons for Miscellaneous Model Series

Model Number	Experimental $C_R \times 10^3$	Simple Formula$_3$ $C_R \times 10^3$	Finite Difference $C_R \times 10^3$
4620	0.10	0.28	0.19
4935	0.11	0.22	0.19
5290	0.15	0.15	0.17
4627	0.20	0.23	0.19
5224-1	0.26	0.16	0.18

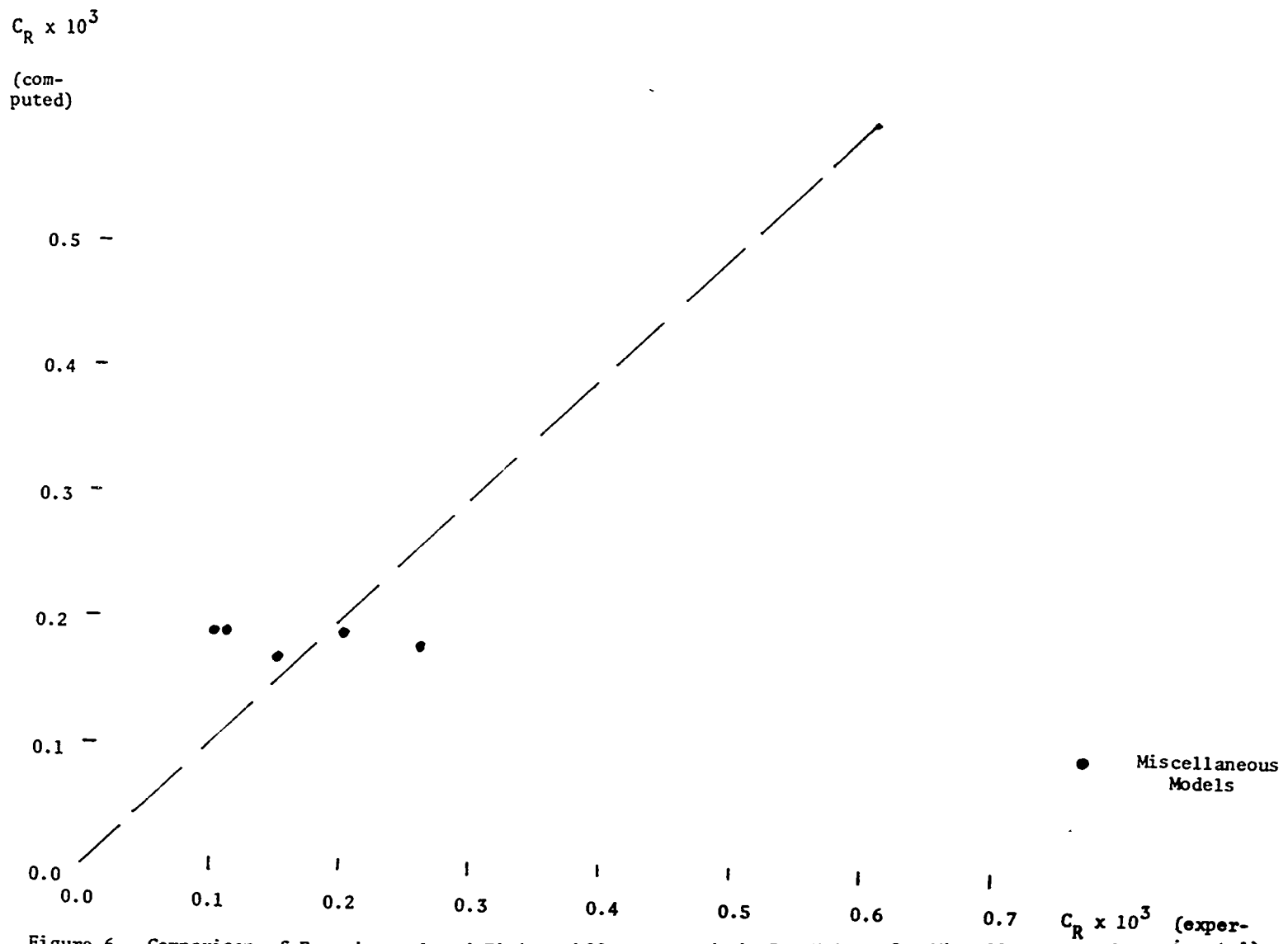

Figure 6. Comparison of Experimental and Finite-Difference-Method C_R Values for Miscellaneous Models.

between the models of this series and predicts an opposing trend for C_R since it increases with increasing L_R/D. The finite-difference method does predict the same trend for C_R as it did for the Series 5242 L_R/D variations.

Kempf Model Series

The seventh series studied consisted of six bodies of revolution having hemispherical noses and sinusoidal sterns of varying fullnesses which were initially investigated by Kempf.[9,10] Sketches, pressure distributions and additional information on these bodies can be found in Reference 5. Computed and measured drag values for this series are shown in Table 13 and Figure 8 graphically compares the results of the finite-difference calculations with the published experimental C_R's.

TABLE 13

Residual Drag Comparisons for the Kempf Body Series

Model Number	$L_{R/D}$	Experimental $C_R \times 10^3$	Simple Formula[3] $C_R \times 10^3$	Finite Difference $C_R \times 10^3$
I	3.00	0.07	0.20	0.16
II	2.50	0.14	0.20	0.25
III	2.00	0.20	0.21	0.27
IV	1.50	0.30	0.21	0.32
V	1.25	0.42	0.26	0.35
VI	1.00	0.75	0.23	0.51

Both the experimental data and the finite-difference method show decreasing C_R's with increasing L_R/D. With the exception of Model VI, the simple formula also indicates this trend. The simple formula does not predict the very large experimental increase of C_R values with decreasing stern fineness, but the finite-difference formula does predict a large increase, albeit not as large as found experimentally. This trend of C_R values is consistent both with the Series 5242 and the Series 4935 variations of L_R/D.

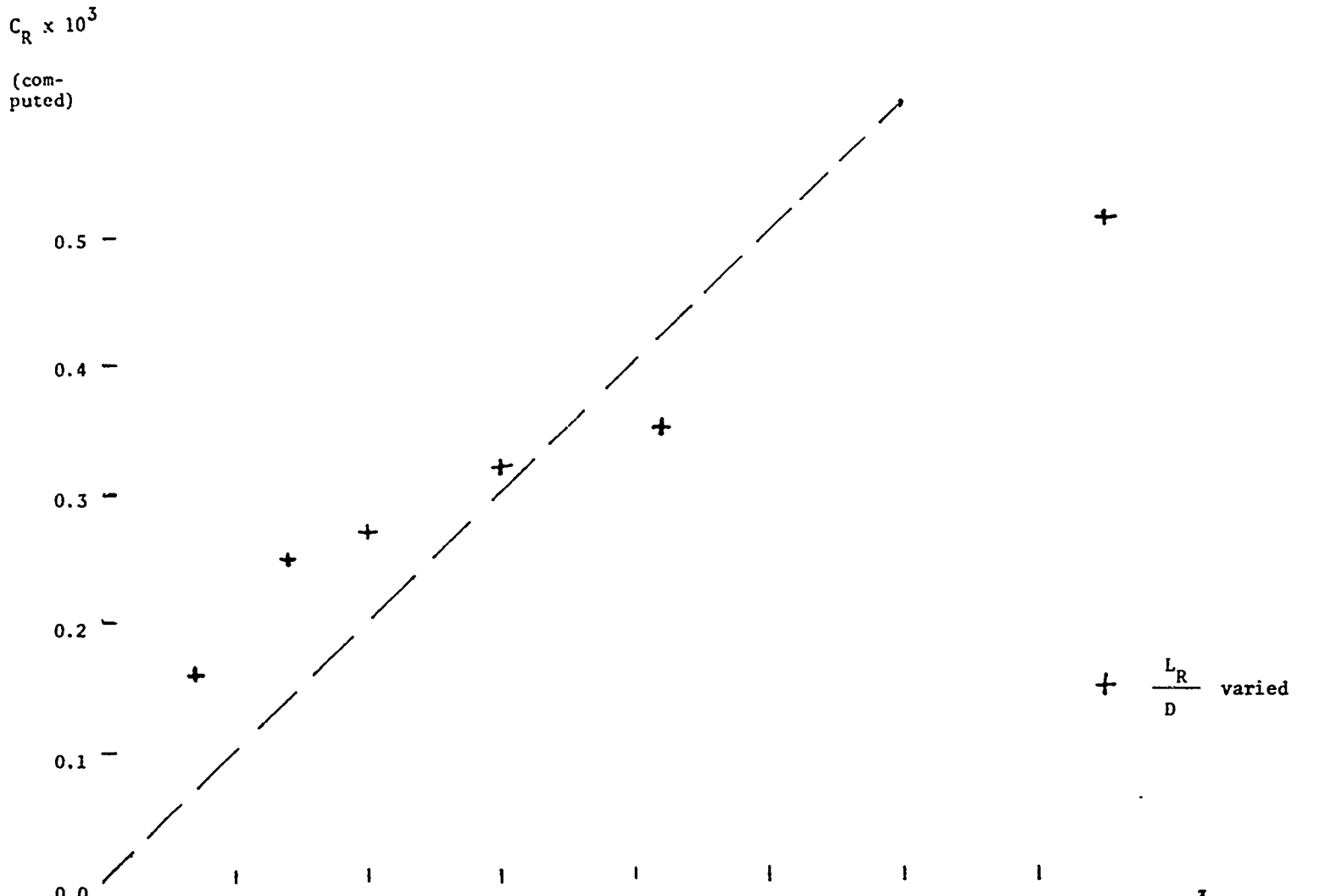

Figure 8. Comparison of Experimental and Finite-Difference-Method C_R Values for Kempf Models.

Series 4620 Afterbodies

The last series of bodies studied was the Series 4620 afterbodies. This series of four stern forms was developed from a parametric study seeking to utilize fuller stern forms and yet maintain unseparated flow over the length of the afterbody. Four types of forms were studied

1) the conventional convex form (Model 4620-3)
2) A short convex tail form (Model 4620-10)
3) A long inflected form (Model 4620-11) and
4) A short inflected form (Model 4620-12).

These models, along with the shape changes, are basically variations on L_R/D made to the tail form of the parent 4620 model studied in the miscellaneous models series. Various amounts of parallel middle body were added to the new tail forms to create four bodies with constant volume equal to that of the parent form. C_p was also varied slightly to see if improvement in the overall performance could be made. The results of the computer calculations are shown in Table 14 below for the finite-difference method only since this series had not been developed when the simple formula was being tested. Figure 9 illustrates graphically the differences between predicted C_R's and the experimental values.

TABLE 14

Residual Drag Comparisons for the Series 4620 Afterbodies

Model Number	C_p	$L_{R/D}$	Experimental $C_R \times 10^3$	Finite Difference $C_R \times 10^3$
4620-3	0.562	4.4	0.15	0.15
4620-10	0.574	2.511	0.16	0.18
4620-11	0.480	3.161	0.21	0.19
4620-12	0.480	3.0315	0.23	0.28

Both the experimental data and the finite-difference method show the same trend in the values of C_R, with the conventional tail and short convex tail rating better than either inflected tail model. In addition, consistent

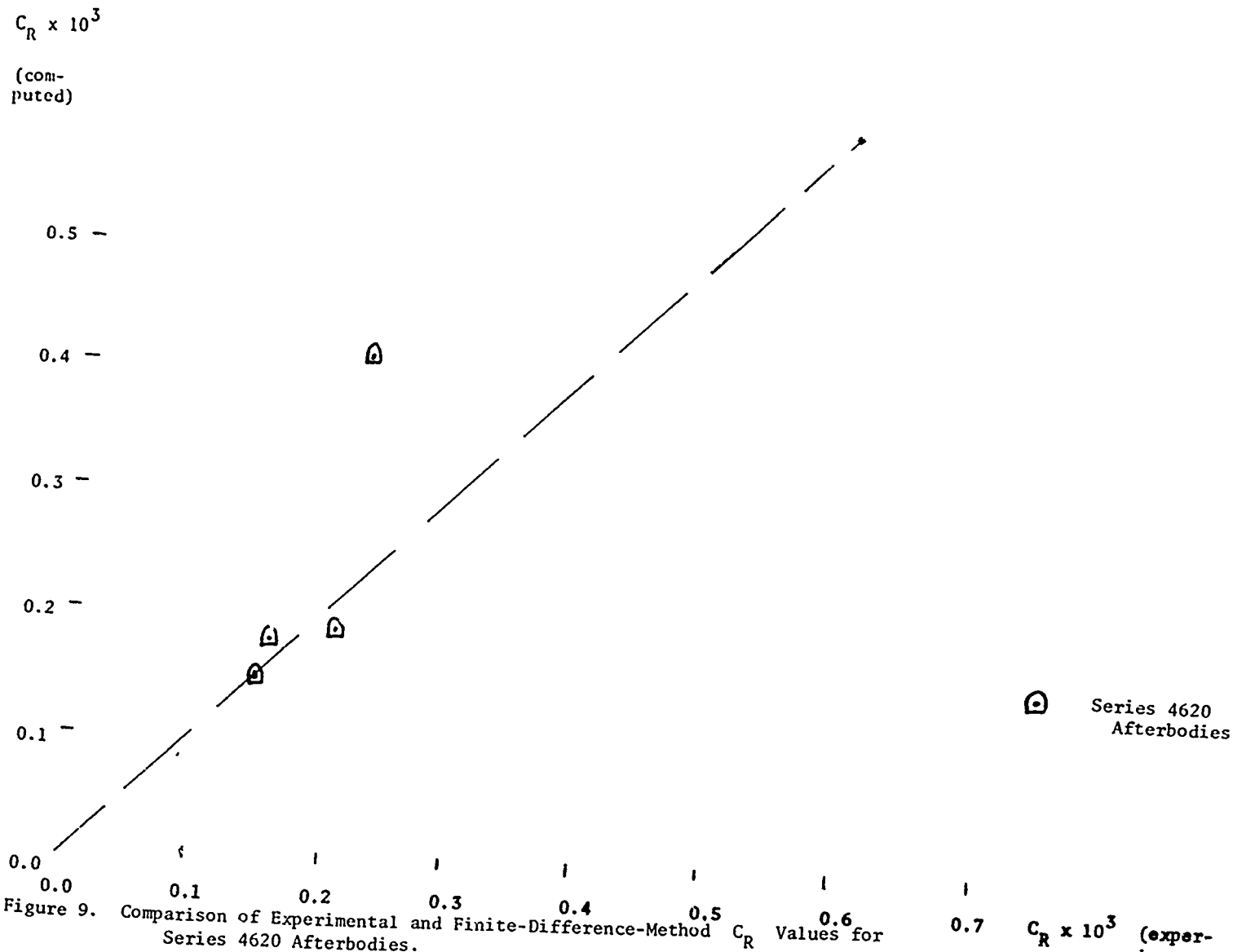

Figure 9. Comparison of Experimental and Finite-Difference-Method C_R Values for Series 4620 Afterbodies.

with other L_R/D variations, both the experimental data and predicted C_R's indicate the long inflected tail (Model 4620-11) has a lower C_R than the short inflected tail. The computer program predicted separated flow for Model 4620-12, which possibly accounts for the large difference between the experimental value of C_R and that predicted by the finite difference method.

CONCLUSIONS

The finite-difference method produced mixed results in this study. The computed drag coefficients show very little sensitivity to such parameters as C_p, m_1, r_o, and r_1. Nor does the finite difference m thod appear to be able to discriminate between bodies where many parameters are varied at the same time, although for the entire tail-shape variations of the series 4620 afterbodies it did predict the correct trend. The program,however, does appear to be able to handle variations in L/D, L_R/D and L_E/D with some success. Trends predicted are correct according to available published data even where exact correlation with experimental values does not occur.

REFERENCES

1. Wang, H.T. and T.T. Haung, "User's Manual for a FORTRAN IV Computer Program for Calculating the Potential Flow/Boundary Layer Interaction Axisymmetric Bodies," DTNSRDC SPD-737-01 (Dec 1976).

2. Cebeci, T., G.J. Mosinskis, and A.M.O. Smith, "Calculation of Viscous Drag and Turbulent Boundary-Layer Separation on Two-Dimensional and Axisymmetric Bodies in Incompressible Flows," Douglas Aircraft Company Report MDC-J0973-01 (Nov 1970).

3. Cebeci, T., G.J. Mosinskis and L.C. Wang, "A Finite Difference Method for Calculating Compressible Laminar and Turbulent Boundary Layers, Part II - User's Manual," Douglas Aircraft Co. Report DAC-671 31 (May 1969).

4. Granville, P.S., "The Calculation of the Viscous Drag of Bodies of Revolution," DTMB Report 849 (Jul 1953).

5. Huang, T.T., et al., "Propeller/Stern/Boundary Layer Interaction on Axisymmetric Bodies: Theory and Experiment," DTNSRDC Report 76-0113 (Dec 1976).

6. White, N.M., "A Comparison Between a Simple Drag Formula and Experimental Drag D-ta for Bodies of Revolution" DTNSRDC Report 77-0028 (Jan 1977).

7. Gertler, Morton, "Resistance Experiments on a Systematic Series of Streamlined Bodies of Revolution - For Application to the Design of High Speed Submarines," DTMB Report C-297 (Apr 1950), declassified 27 Jan 1967.

8. Larsen, C.A., "Additional Tests of Series 58 Forms, Part 1, Resistance Tests on a Parallel Middle Body Series," DTMB Report C-738 (Nov 1955), declassified 2 Sept 1975.

9. McCarthy, J.H., J. Power, and T.T. Huang, "The Roles of Transition, Laminar Separation and Turbulence Stimulation in the Analysis of Axisymmetric Body Drag," Proceedings of the Eleventh ONR Symposium on Naval Hydrodynamics, sponsored by the Office of Naval Research, London (Mar 1976).

10. Kempf, George, "Resistance and Wake of Some Bodies of Revolution" from "New Developments in Ship Research", Jahrbuch Schiffbautechnischen Gesellschaft (1927), pp. 177-178.

11. Kempf, George, "Turbulent Sepearation on Full Ship Forms," Schiff und Hafen, Vol. 6, no. 7, Hamburg (1954).

DTNSRDC ISSUES THREE TYPES OF REPORTS

(1) DTNSRDC REPORTS, A FORMAL SERIES PUBLISHING INFORMATION OF PERMANENT TECHNICAL VALUE, DESIGNATED BY A SERIAL REPORT NUMBER.

(2) DEPARTMENTAL REPORTS, A SEMIFORMAL SERIES, RECORDING INFORMATION OF A PRELIMINARY OR TEMPORARY NATURE, OR OF LIMITED INTEREST OR SIGNIFICANCE, CARRYING A DEPARTMENTAL ALPHANUMERIC IDENTIFICATION.

(3) TECHNICAL MEMORANDA, AN INFORMAL SERIES, USUALLY INTERNAL WORKING PAPERS OR DIRECT REPORTS TO SPONSORS, NUMBERED AS TM SERIES REPORTS; NOT FOR GENERAL DISTRIBUTION.